

Homeostatic conductance regulation in multicompartment model neurons

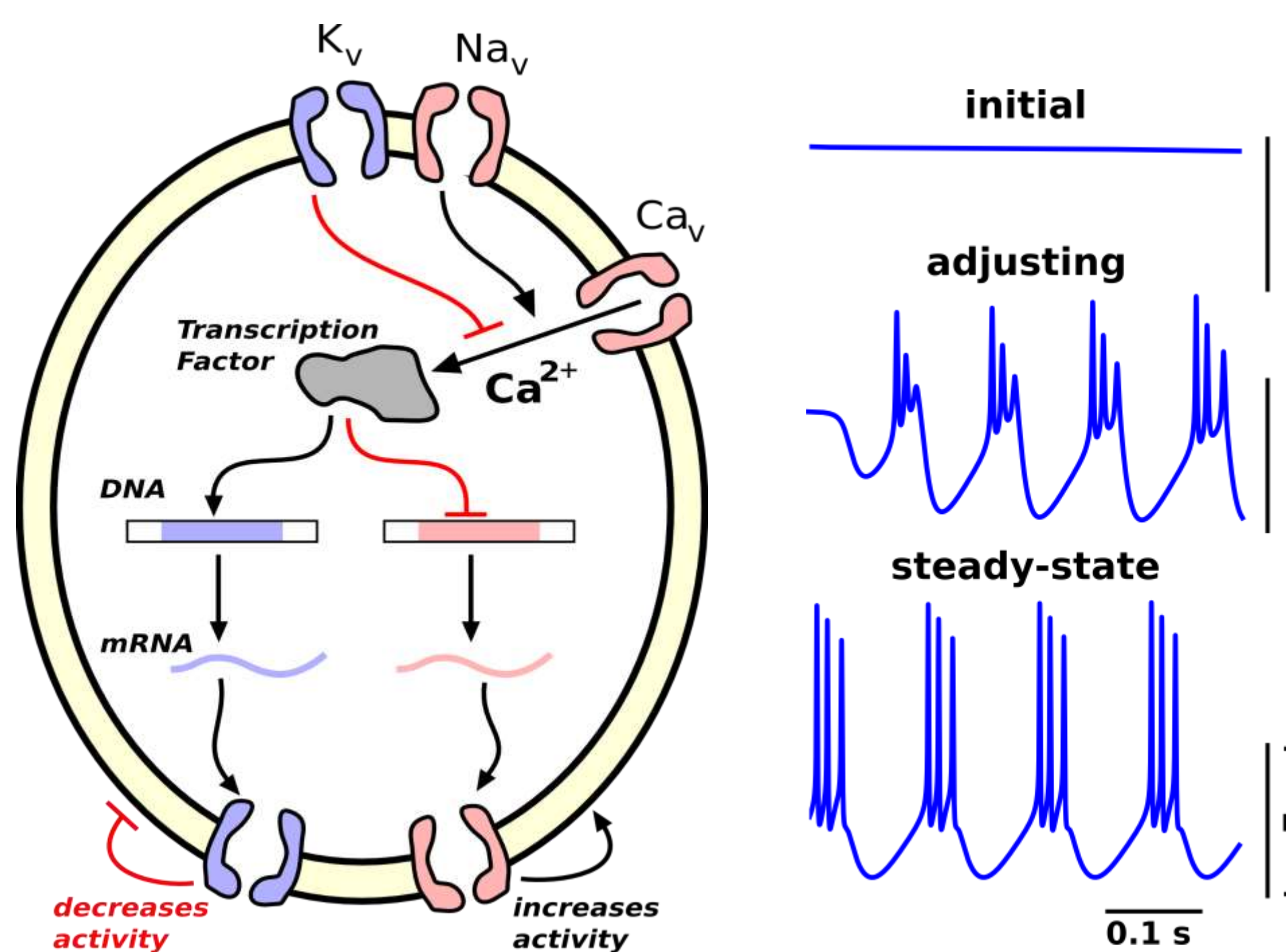
Alex H. Williams*, Timothy O'Leary, Eve Marder

Department of Biology, Brandeis University, Waltham MA.

*Current Affiliation: Department of Neuroscience, UC San Diego, La Jolla CA

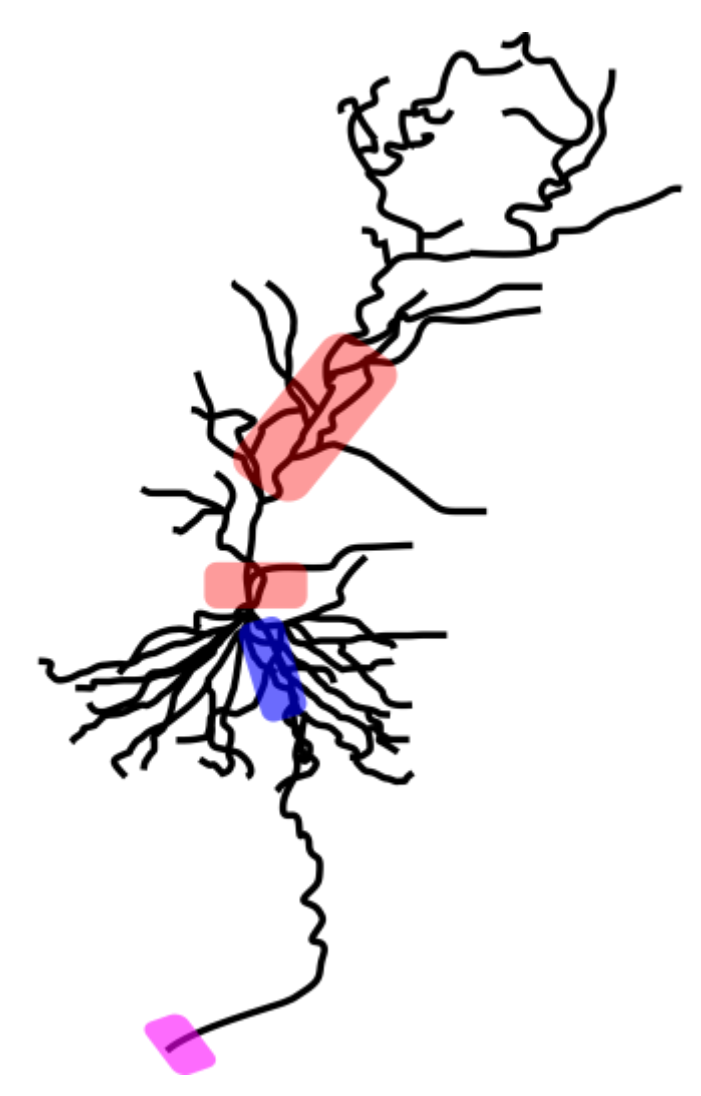
Background

- Feedback control systems keep physiological variables within desired ranges (e.g. *thermoregulation, blood glucose levels*)
- Neurons use similar principles to regulate their activity patterns (e.g. to maintain average firing rates; Hengen et al, 2013)



Models for homeostatic plasticity work well in single-compartment. Above, an activity-dependent conductance regulation rule with negative feedback (*left*) produces a self-organizing bursting cell (*right*), which is robust to perturbations (O'Leary et al., 2014)

But how can homeostatic feedback be incorporated into multicompartment models?



Homeostatic plasticity occurs in sub-cellular domains:

- Dendrites**
Ex: *Npas4* differentially regulates inhibition onto apical dendrites and soma (Bloodgood et al., 2013)
- Pre-synaptic terminals**
Ex: AMPAR blockade increases vesicle pool size (Thiagarajan et al., 2013)
- Axon initial segment**
AIS shifts away from soma following hyperactivity (Grubb & Burrone, 2010)

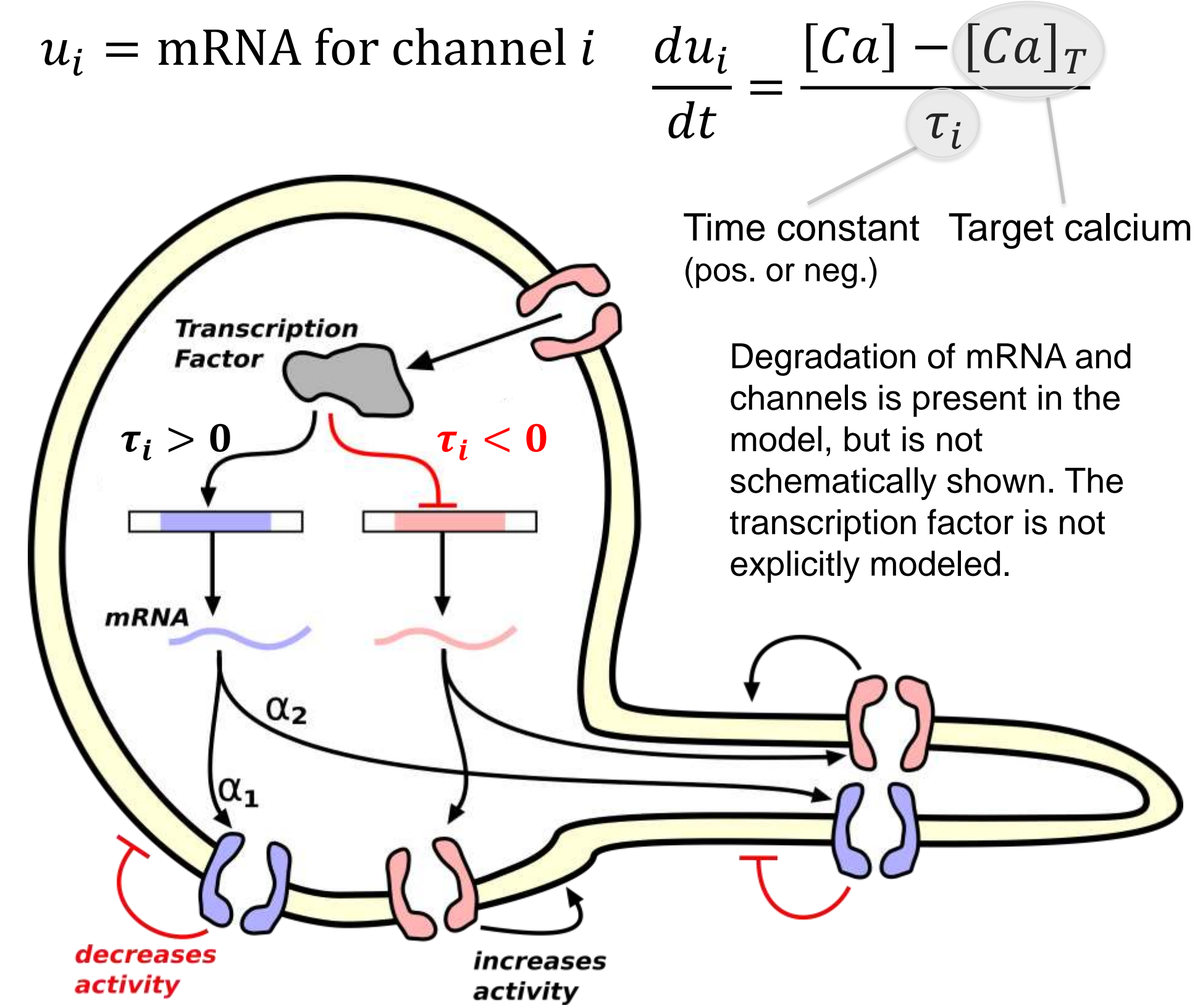
Problems of interest:

- Components of feedback system (sensors, actuators, etc.) are spatially separated**
- Competition between local and global regulation rules (e.g. LTP and synaptic scaling)**
- Rules for trafficking proteins and mRNA involved in plasticity between sub-cellular compartments**

Case #1:

mRNA production/trafficking is much faster than channel translation/insertion

mRNA reaches a steady-state distribution across compartments rapidly. Easy to extend O'Leary et al. (2014):



Equations for changes in maximal conductance:

$$\frac{d\tilde{g}_{i,s}}{dt} = \alpha_{i,s}u_i - \beta_{i,s}\tilde{g}_{i,s} \quad \tilde{g}_{i,s} = \tilde{g}_{i,s}/A_s$$

channel insertion & trafficking bias degradation rate constant surface area

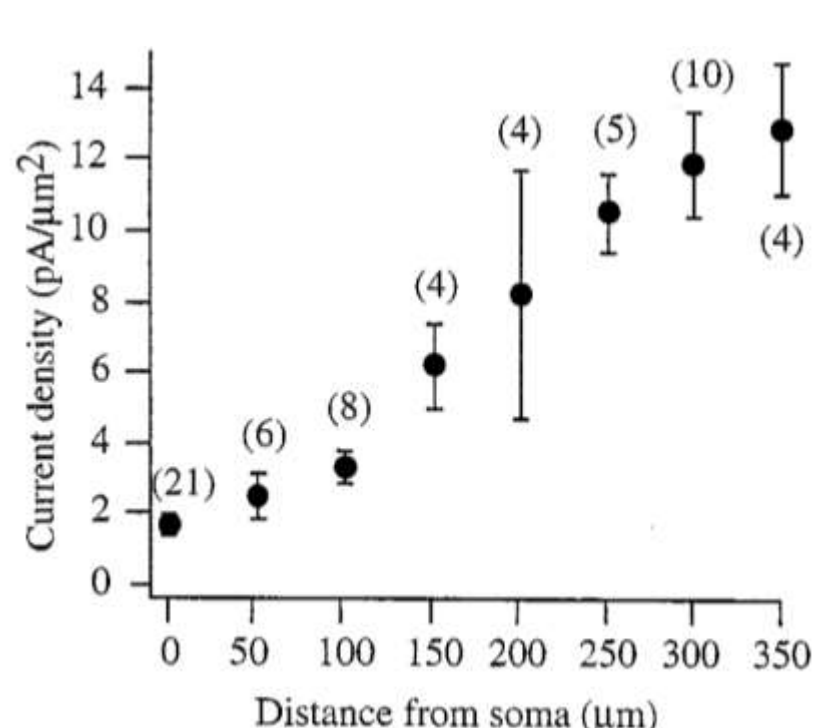
Experimental Prediction: If we assume $\tilde{g}_i \approx 0$ for the initial condition of the simulation (e.g. an early stage of neural development), then we observe **consistent ratios in channel expression between compartments** across preparations. Similar results were used by O'Leary et al. (2014) to explain correlations *between channel types* across preparations (see, e.g., Schulz et al., 2007)

$$\frac{\tilde{g}_{i,s_1}|_{ss}}{\tilde{g}_{i,s_2}|_{ss}} \approx \frac{\left(\frac{\alpha_{i,s_1}u_i|_{ss}}{\beta_{i,s_1}}\right)}{\left(\frac{\alpha_{i,s_2}u_i|_{ss}}{\beta_{i,s_2}}\right)} = \frac{\alpha_{i,s_1}\beta_{i,s_2}}{\alpha_{i,s_2}\beta_{i,s_1}} \times \frac{A_{s_2}}{A_{s_1}}$$

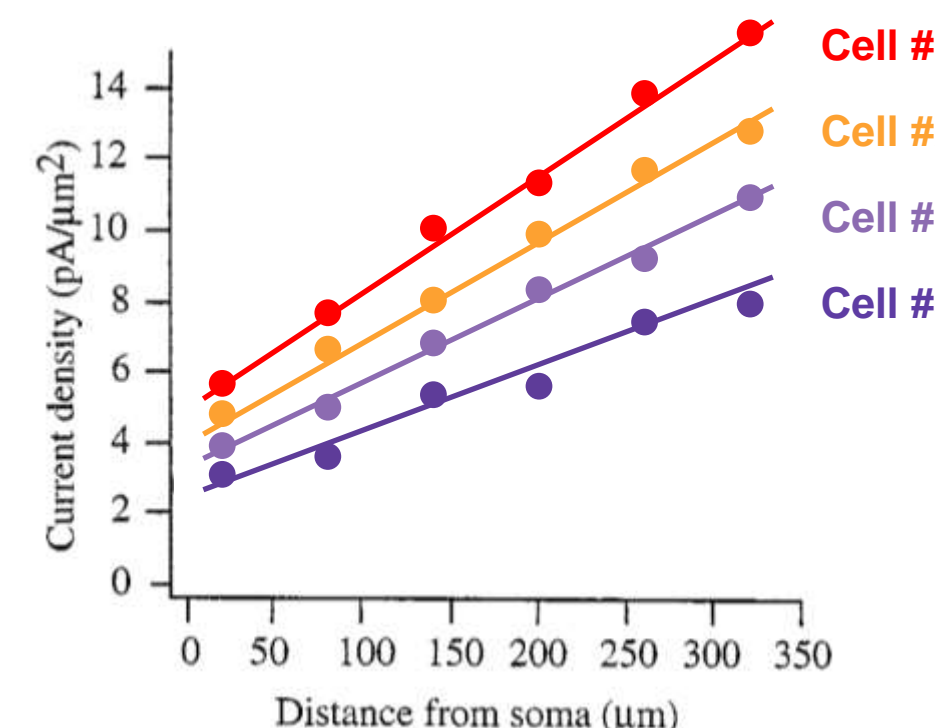
Significance:

- Experimentally measure conductance ratios to determine homeostatic parameters in real neurons
- Develop homeostatic versions of static models by deriving regulation parameters from $\tilde{g}_{i,s}$

Average I_H gradient
Magee et al. (1999)



Individual I_H gradients
(schematic, predicted)



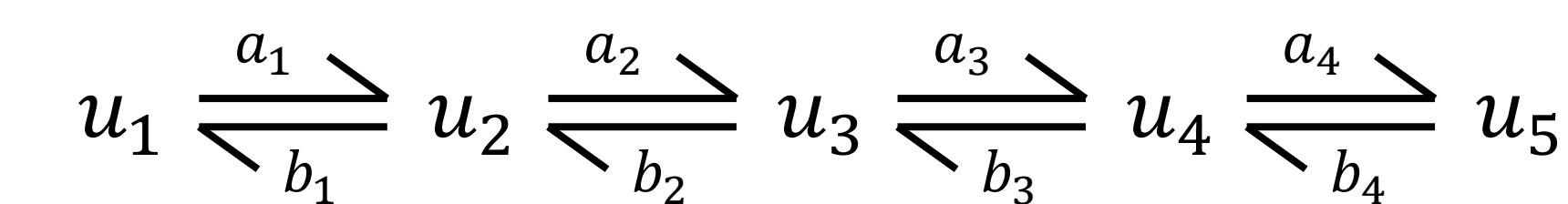
Case #2: Modeling mRNA trafficking explicitly

iPad goes here for animations

http://nbviewer.ipynb.org/github/ahwillia/notebooks/tree/master/code_pubs/2014_11_04/trafficking.ipynb

Simple case: a linear cable

Model mRNA movement using mass action kinetics with rate constants a_i and b_i



$$\frac{du_i}{dt} = a_{i-1}u_{i-1} + b_iu_{i+1} - (a_i + b_{i-1})u_i$$

$$\dot{\mathbf{u}} = \mathbf{A}\mathbf{u} \quad \mathbf{A} \text{ is a tridiagonal matrix}$$

Goal: Choose a_i and b_i such that mRNA approaches a desired distribution $\mathbf{u}_{i,ss} = \tilde{\mathbf{u}}_i$

Solution:

$$\frac{a_i}{b_i} = \frac{\tilde{u}_{i+1}}{\tilde{u}_i}$$

To see why, solve by substitution:

$$a_{i-1}\tilde{u}_{i-1} + b_i\tilde{u}_{i+1} - (a_i + b_{i-1})\tilde{u}_i = 0$$

$$a_{i-1}\tilde{u}_{i-1} + b_i\tilde{u}_{i+1} = a_i\tilde{u}_i + b_{i-1}\tilde{u}_i$$

$$\frac{\tilde{u}_i}{\tilde{u}_{i-1}} b_{i-1}\tilde{u}_{i-1} + b_i\tilde{u}_{i+1} = \frac{\tilde{u}_{i+1}}{\tilde{u}_i} b_i\tilde{u}_i + b_{i-1}\tilde{u}_i$$

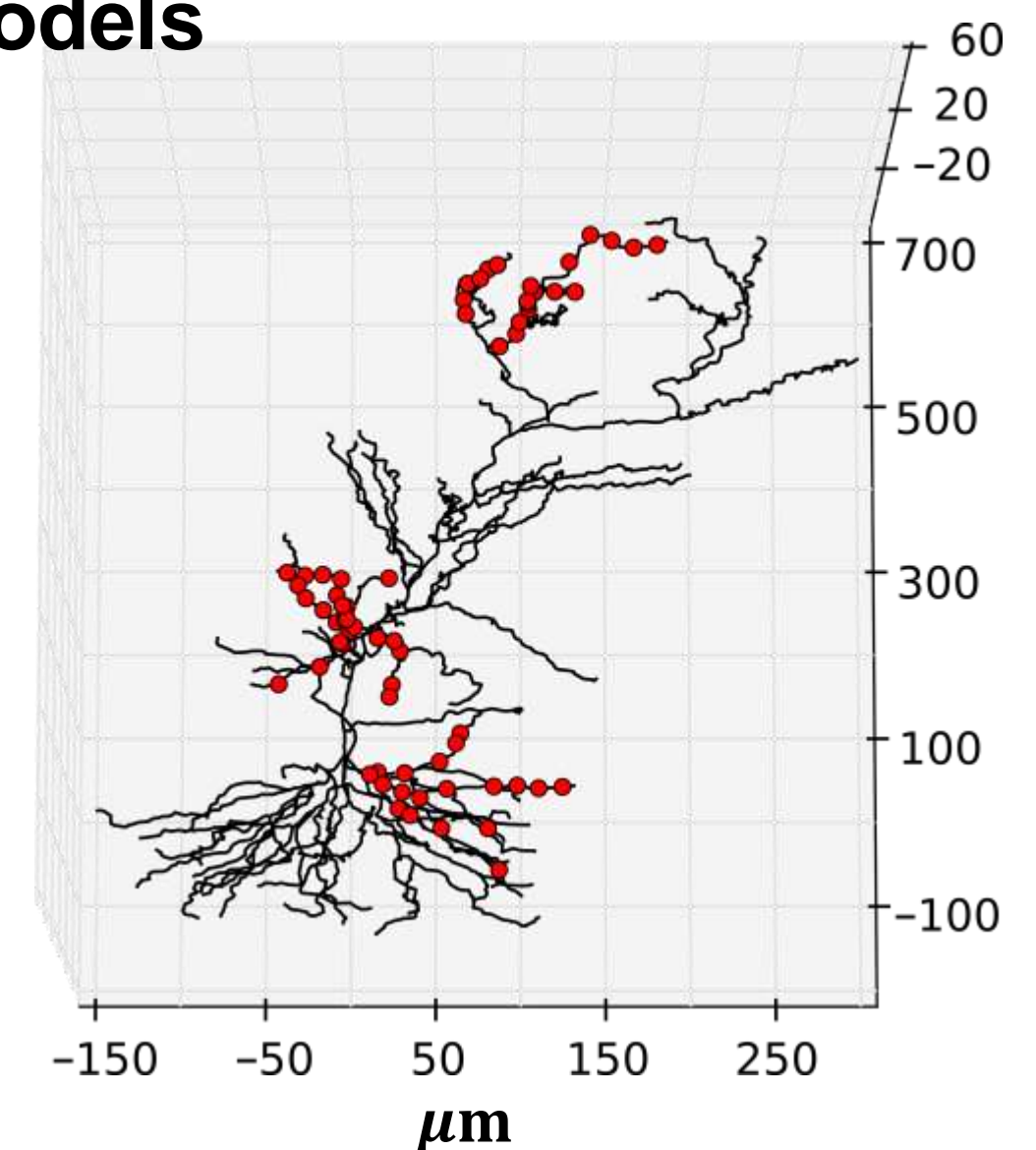
$$b_{i-1}\tilde{u}_i + b_i\tilde{u}_{i+1} = b_i\tilde{u}_{i+1} + b_{i-1}\tilde{u}_i$$

This works for any branched morphology and any target distribution as long as all $\tilde{u}_i > 0$

Code and animations available at: http://nbviewer.ipynb.org/github/ahwillia/notebooks/tree/master/code_pubs/2014_11_04/trafficking.ipynb

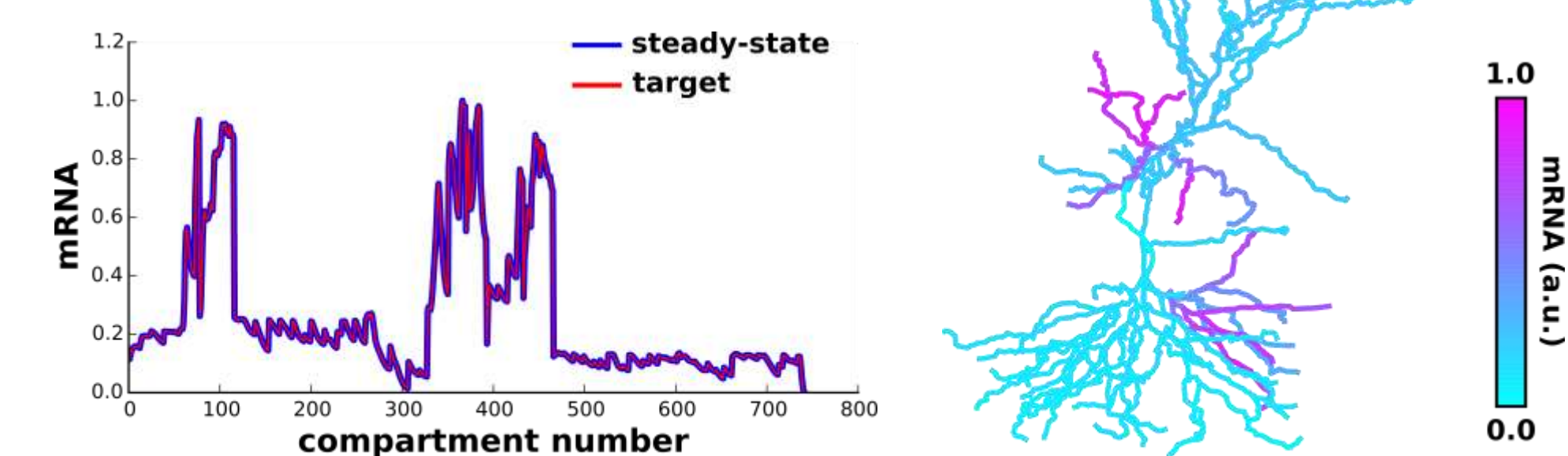
Activity-dependent trafficking in realistic multicompartment models

- Model CA1 pyramidal cell (Migliore & Migliore, 2012). Uses NEURON simulator.
- Excitatory synapses at red dots in figure, firing at 50 Hz.
- Plots made using PyNeuron Toolbox (Williams, 2014)



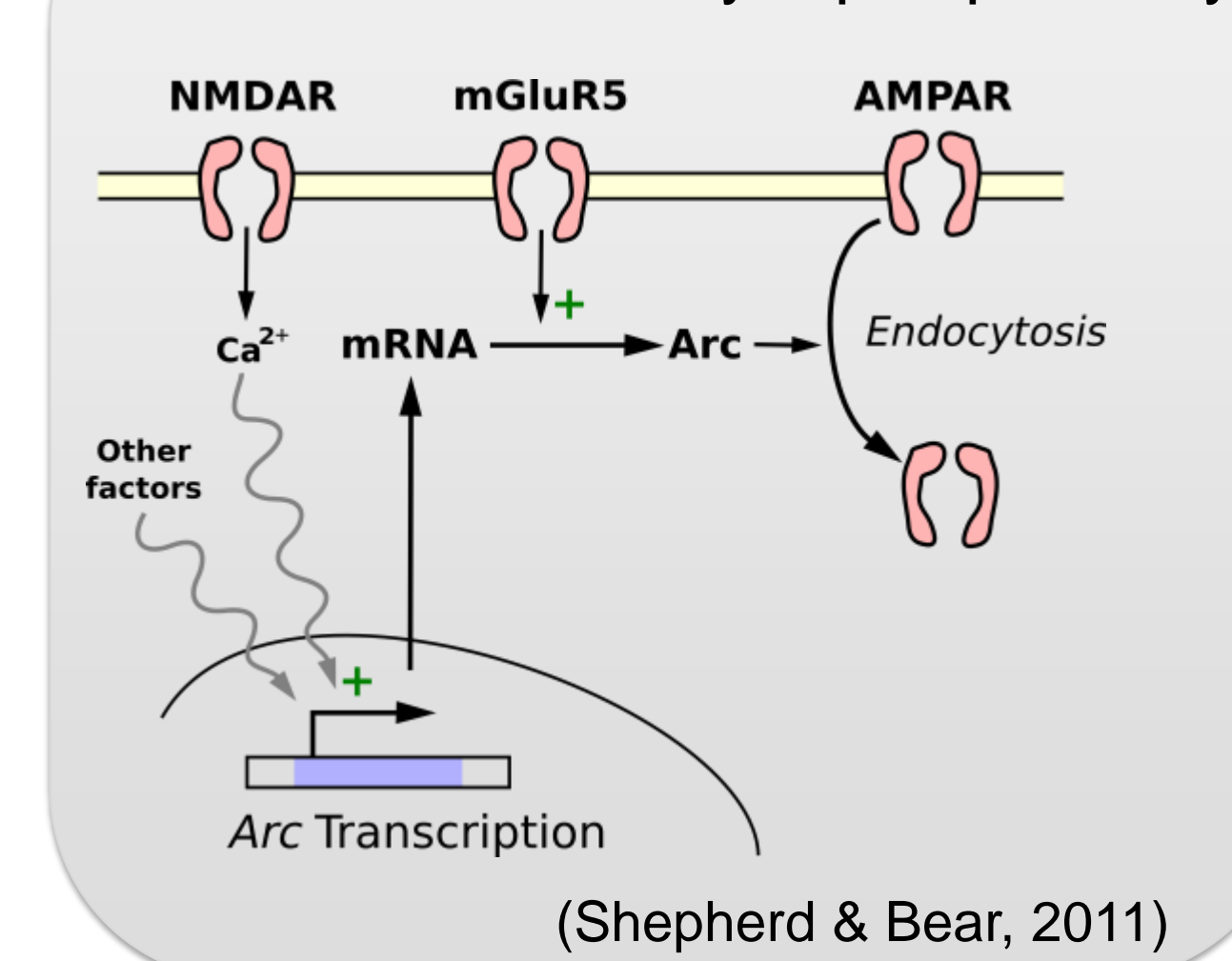
Dynamic and reversible trafficking rules

- A local signal tied to activity (e.g. Ca^{2+}) can be used to define \tilde{u}_i .
- mRNA accumulates at active synaptic sites. The steady-state distribution (*right*) exactly matches the desired outcome (*below*).



Preliminary work: Interactions between local and global regulation

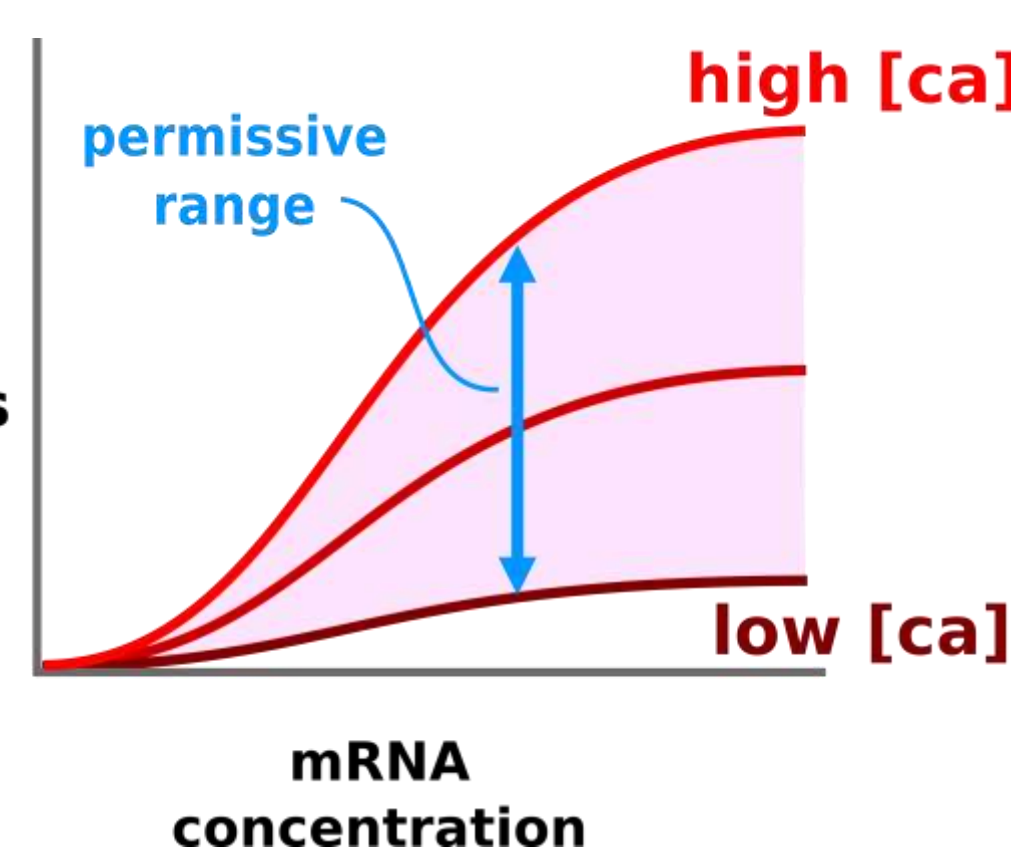
Ex: Arc-mediated synaptic plasticity



$$\frac{d\tilde{g}_{i,s}}{dt} = \alpha_{i,s}([Ca]_s, u_i) - \beta_{i,s}\tilde{g}_{i,s}$$

$$\tilde{g}_{i,s}|_{ss} \approx \frac{\langle \alpha_{i,s}([Ca]_s, u_i) \rangle}{\beta_i}$$

We can model $\alpha_{i,s}$ as a function of local calcium concentration and mRNA expression. Local calcium signals up or down regulate maximal conductance within a permissive range (*blue line in schematic plot*). This range is regulated by global activity through activity-dependent transcription. Arc is an example of a gene whose transcription is controlled by global activity levels and whose trafficking/translation are regulated by local activity (*see box on left*).



Bloodgood BL*, Sharma N*, Browne HA, Trepman AZ, Greenberg ME, Domain-specific regulation of inhibitory synapses by the activity-dependent transcription factor Npas4. *Nature*, 2013 Nov 7. 503(7474):121-5.

Grubb GS, Burrone J (2010). Activity-dependent relocation of the axon initial segment fine-tunes neuronal excitability. *Nature*. 465(7301):1070-4.

Hengen K, Lambo ME, Van Hooser SD, Katz DB, and Turrigiano GG (2013). Firing rate homeostasis in visual cortex of freely behaving rodents. *Neuron*. 80(2):335-42.

Magee JC (1999). Dendritic I_H normalizes temporal summation in hippocampal CA1 neurons *Nat Neurosci*. 2, 508-14

Migliore M, Migliore R (2012) Know your current I : interaction with a shunting current explains the puzzling effects of its pharmacological or pathological modulations. *PLoS One* 7(5):e36867

O'Leary T, Williams AH, Franci A, Marder E (2014). Cell types, network homeostasis and pathological compensation from a biologically plausible ion channel expression model. *Neuron*. 82(4):809-21.

Shepherd & Bear (2011). New views of Arc, a master regulator of synaptic plasticity. *Nat Neurosci*. 14(3):279-284

Schulz DJ, Goaillard J-M, Marder E (2007) Quantitative expression profiling of identified neurons reveals cell-specific constraints on highly variable levels of gene expression. *Proc Natl Acad Sci*, USA 104: 13187-13191.

Thiagarajan TC, Lindskog M, Tsien RW (2005). Adaptation to synaptic inactivity in hippocampal neurons. *Neuron*. 47(5):725-37.

Williams AH (2014). PyNeuron Toolbox. *GitHub Repository*. <https://github.com/ahwillia/PyNeuron-Toolbox>

Support: NIH Grant 1P01NS079419, Charles A. King Trust, Department of Energy Computational Science Graduate Fellowship.